J Mater Sci (2009) 44:2497–2506
DOI 10.1007/s10853-009-3320-3

Flexural and low-cycle fatigue behavior of atmospheric ice

Majid Kermani · Masoud Farzaneh

Received: 31 August 2008 / Accepted: 4 February 2009 / Published online: 5 March 2009

Abstract Accretion of atmospheric ice on power transmission lines may have detrimental effects, sometimes with major socio-economical consequences. The mechanical behavior of this type of ice as an important aspect in the understanding of that issue is still unclear. In the present study, more than 70 tests were conducted using cantilever beams under gradually increasing cyclic load to measure the bending strength of various types of atmospheric ice. Atmospheric ice was accumulated in a closed-loop wind tunnel at −6, −10, and −20 °C, with a liquid water content of 2.5 g m^{-3}. Ice samples accumulated at each temperature level were tested at the accumulation temperature, but the ice accumulated at −10 °C was also tested at −3 and −20 °C. Compared to the bending strength results for atmospheric ice under static load, the ice showed less resistance against fracture under cyclic load. It was also revealed that bending strength of atmospheric ice decreases with the test temperature. Another 60 samples of atmospheric ice were also tested under cyclic loads with constant amplitude. The tests revealed that the samples of atmospheric ice accumulated at −10 and −6 °C do not fail under stresses less than 1 MPa after 2000 cycles. At stress levels close to the bending strength of atmospheric ice, however, sometimes the specimen fails after a few hundred cycles. In comparison with the ice accumulated at −10 and −6 °C, atmospheric ice accumulated at −20 °C fails at stresses less than its bending strength. This can be attributed to the colder test temperature and the presence of cavities and cracks in this ice that reduce its bending strength during cyclic stresses.

M. Kermani (✉) · M. Farzaneh
NSERC/Hydro-Québec/UQAC Industrial Chair on Atmospheric Icing of Power Network Equipment (CIGELE), and Canada Research Chair on Atmospheric Icing Engineering of Power Networks (INGIVRE), Université du Québec à Chicoutimi, Chicoutimi G7H 2B1, Canada
e-mail: mkermani@uqac.ca
URL: www.cigele.ca

Introduction

The accumulation of atmospheric ice on power transmission lines is a source of major damage to power networks. It is common knowledge that in cold regions significant ice layers may accumulate on cables and conductors. This accumulation can produce major problems, such as overloading the conductors and towers, galloping of cables in high wind conditions, ice shedding, short-circuits due to wire sag, etc. Ice shedding is the name given to the physical phenomenon that occurs when the accreted ice suddenly drops off of the cables, either naturally or as a result of some form of intervention. Removing the atmospheric ice from network equipment, particularly cables and conductors has drawn much attention lately, and consequently, many studies on ice adhesion on substrates, ice shedding and its effects on power network elements have been carried out (e.g. Javan-Mashmool et al. [1], Eskandarian [2], Jamaleddine et al. [3]). The most important mechanical property of atmospheric ice that plays a key role in ice removal and ice shedding is its bending strength. The low-cycle fatigue behavior of this ice also plays an important role during cyclic loads. These properties of atmospheric ice determine its resistance against fracture and shedding during galloping and aeolian vibration of power transmission lines. Therefore, the above-mentioned properties are topics of general interests in de-icing studies and modeling of ice shedding.

The present investigation is part of a larger study on the measurement of the mechanical properties (compressive strength, bending strength, fracture toughness, etc.) of atmospheric ice, yet to be published.

The sole study on the bending strength of atmospheric ice is the research of Kermani et al. [4], where the specimens of atmospheric ice were used as three-point simple support beams in push-down mode with various load rates. The results of that research are compared with those of this study which were carried out under cyclic loads (push-down and pull-up mode).

Many other investigators studied the flexural properties of other types of ice (e.g. Timco and Frederking [5], Frederking and Svec [6], Dempsey et al. [7], Gow and Ueda [8], Gagnon and Gammon [9]). The dynamic failure of ice and the effects of impact on mechanical behavior of ice have been studied by other researchers (e.g. Kim and Keune [10], Gagnon [11]). A considerable amount of work has also been done on the fatigue of fresh water ice and sea ice (e.g. Haynes et al. [12], Nixon and Smith [13], Haskell et al. [14], Weber and Nixon [15], Nixon and Weber [16]). However, to the best of our knowledge, the present study is the first attempt at investigating the low-cycle fatigue behavior of atmospheric ice.

Specimen preparation

Atmospheric ice and its structure can be influenced by the meteorological conditions prevalent during its formation, such as wind velocity, liquid water content of air, mean volume droplet diameter, and temperature. Furthermore, the mechanical properties of atmospheric ice are dependent on temperature, load rate, ice type, and structure. Therefore, the most important aspect in this investigation is selecting the experimental conditions for the ice accumulation and ice tests, which is discussed in the following paragraphs.

The ice accumulation conditions for this study were created in the CIGELE[1] atmospheric icing research wind tunnel which is a closed-loop (air-recirculated) low-speed icing wind tunnel. Icing conditions, as those encountered during various icing processes in nature, can be simulated in this tunnel. The characteristics of ice accumulation equipment have been discussed in Kermani et al. [17]. Air speed that typically leads to natural glaze ice formation ranges from ultra low to medium speeds. In order to make the experimental work more manageable and obtain a more uniform ice layer, an air velocity value of 10 ms^{-1} was chosen.

Three ambient temperature values, −6, −10, and −20 °C, were selected for the accumulation of atmospheric ice as representative of warm, medium, and cold icing conditions.

It was assumed that air pressure was equal to 1 NACA standard atmosphere at sea level (P_{st} = 101325 Pa), and that relative humidity ranged from 0.81%–0.92%.

Liquid water content (LWC) of the CIGELE wind tunnel depends on the difference between air and water line pressures, air speed and the flow rate of water in the supply line. It was calibrated as a function of the aforementioned parameters by Kollár and Farzaneh [18]. LWC for icing conditions in nature varies between 0.5 and 10 g m^{-3}, which is within the range of the wind tunnel. During the calibration, LWC at the test section of the wind tunnel was measured using the accepted standard technique known as the rotating icing cylinder method [19]. So, LWC was set at 2.5 g m^{-3} in order to obtain solid and uniform atmospheric ice.

Atmospheric ice was accumulated on an aluminum cylinder (diameter 78 mm and length 590 mm) placed in the middle of the test section of the wind tunnel and rotated at a constant speed of 2 rev min^{-1}. Before ice accumulation, the cylinder was cleaned with alcohol and set in place for 2 h while the system was cooling down. Once accumulation was over, the cylinder was removed from the test section and the accumulated ice was cut with a warm aluminum blade to avoid any mechanical stress that might cause cracks. The resulting ice slices were then carefully prepared using a microtome. The average time interval between ice accumulation and flexural tests was 5 h. Figure 1 shows the position of the specimens extracted from the accumulated ice on the cylinder, and the load direction in the mechanical tests.

Specimen dimensions, as mentioned in ASTM E111-97, were determined by averaging three measurements along

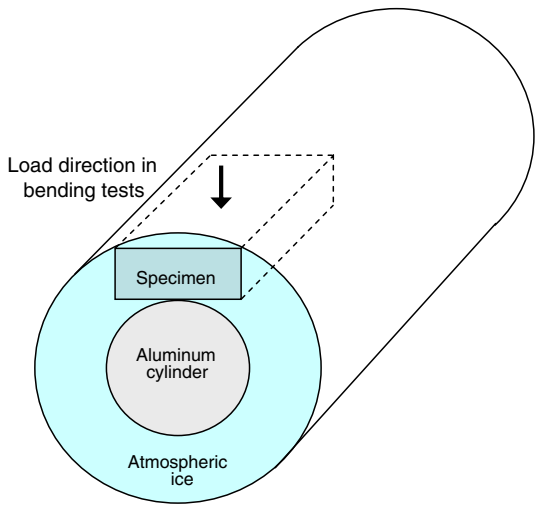

Fig. 1 Specimen position in accumulated atmospheric ice and load direction during test

[1] Industrial Chair on Atmospheric Icing of Power Network Equipment.

the three axes of the samples. In preparing the specimens, the guidelines recommended by the IAHR (International Association of Hydraulic Engineering and Research) working group on test methods [20] were used.

Test conditions

The mechanical behavior of ice can be influenced by test conditions such as temperature, specimen size, loading rate, failure mode, etc. Considering this, the test conditions have been chosen very carefully for this study.

The specimens were accumulated at different temperatures and tested at their accumulation temperatures. However, the atmospheric ice accumulated at the typical wintertime temperature (−10 °C) was tested at three temperatures −3, −10, and −20 °C. The specimens were kept at the test temperature for 2 h before each test.

In these tests, the flexural strength of atmospheric ice was determined using a cantilever beam bending setup with a cyclic load at the end of the beam as a push-down and pull-up load.

According to Schwarz et al. [20], for beams of freshwater ice (whose structure is closest to atmospheric ice) the ratio of beam width to ice crystal size must be ≥10, in order to eliminate the grain size effect. It is also recommended that a beam length 7–10 times that of beam thickness is used. Because of limitations in preparing ice beams of that ratio, a length to thickness ratio of 5 was used. Accordingly, the following dimensions were chosen for our specimens: beam width (w) 40 mm, beam thickness (h) 20 mm, and beam length (L) 100 mm.

A commercial closed-loop, servo-hydraulic material test system (MTS) was used to conduct the tests. The test machine was situated inside a cold room with an observation window. The machine has one actuator and one servo-controller. Both displacement and force controlled tests can be performed. The load and displacement histories (variation of load and displacement with time) can be controlled by setting the desired load or displacement history in the controller software. During testing, the recording system provides an instantaneous graph which shows the history of both the applied load (or displacement) and measured displacement (or load) so that an exact record of the experiment history is known at the time of testing.

As mentioned previously, the purpose of this research is to study the mechanical behavior of atmospheric ice under cyclic loads during galloping of power transmission lines. Kermani [21] developed a model of galloping of cable with accreted atmospheric ice. The load frequency in the present study was set at 0.3 Hz, accordingly with the results of the above-mentioned model for a wind velocity of 5 m s^{-1}. Two different scenarios for the cyclic tests were used. In the first scenario, 71 tests were conducted to measure the bending strength of different types of atmospheric ice during a cyclic load with increasing stress amplitude. The direction of bending force was changed twice during each cycle and its amplitude was gradually increased from a value of zero up to that of beam failure with an increasing rate of 2 N/cycle. In the second scenario, 65 tests were conducted to study the ice fracture due to low-cycle fatigue crack propagation. A cyclic load is termed low-cycle fatigue if the cycle number up to the initiation of a visible crack or until final fracture is below 10^4 or 5.10^4 [22]. During these tests, the effects of a constant and repetitive load on resistance of ice against crack propagation and fracture were investigated.

Grain structure of atmospheric ice

Thin sections of atmospheric ice accumulated at −6 °C (parallel to the cylinder's axis) reveal that the average grain size of this type of ice is approximately 1.5 mm, and varies from 0.5 mm to 3 mm (Fig. 2a). The porosity of ice is defined as the ratio of voids or bubble volume to the total volume of the ice sample. Ice porosity was approximately 2.9% at the accumulation temperature of −6 °C, based on the measured volume and mass of the samples.

The grain size of atmospheric ice accumulated at −10 °C is observed to be considerably smaller than that accumulated at −6 °C (approximately 0.5 mm, Fig. 2b). From this fact, one may conclude that the grain size of atmospheric ice decreases with decreasing deposit temperature, which is in agreement with the observations of Laforte and Phan [23]. According to the measurements of sample mass and volume, the porosity of the ice accumulated at −10 °C was approximately the same as the ice accumulated at −6 °C.

A significant number of cavities, and possibly cracks, are visible in the ice accumulated at −20 °C. The presence of these cavities is attributed to the high freezing rate of the droplets, which prevents them from filling the cavities. Grain size in this type of ice averages less than 0.4 mm, the grain boundaries are more angular than that of the ice accumulated at −10 °C, and the cavities are distinctive (Fig. 2c). Polarized filters were oriented to highlight the grain structure in Fig. 2c, but differently so than in Fig. 2d, where the intention was to highlight cavities. The porosity of this type of atmospheric ice was found to be 8.5%. The higher value of porosity is due to the significant amount of cavities and voids.

A thin section perpendicular to the cylinder axis of the ice accumulated at −10 °C (Fig. 3a) shows that at thicknesses greater than about 2 mm, the grains are elongated

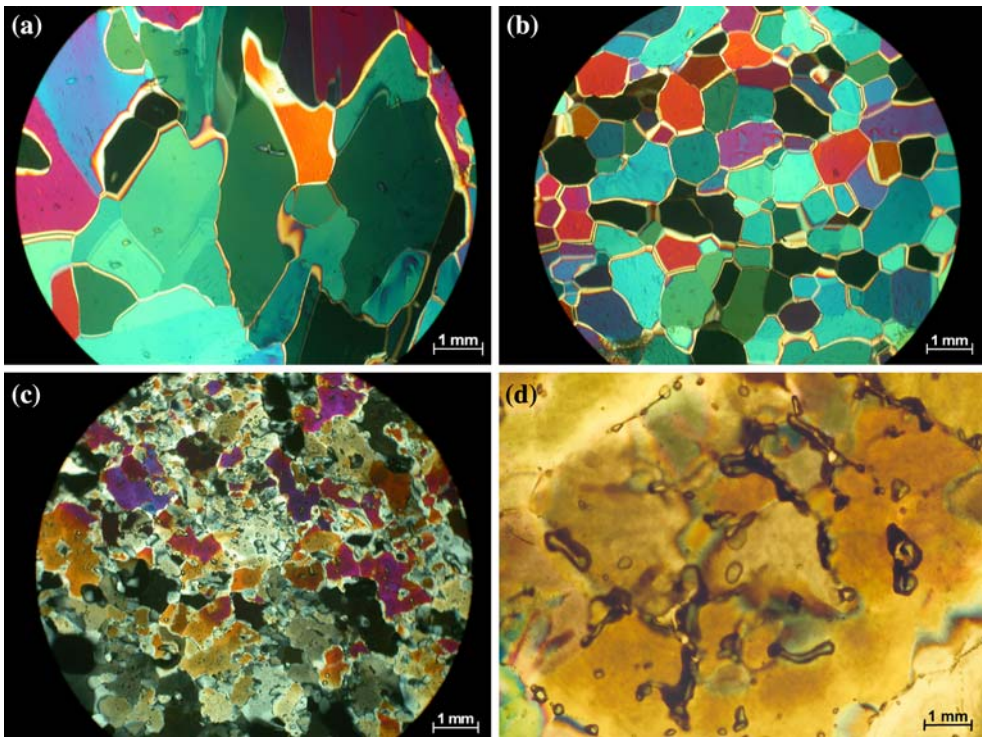

Fig. 2 Thin section (parallel to the cylinder axis) of ice accumulated at **a** −6 °C, **b** −10 °C, **c** −20 °C, **d** Thin section showing cavities and possibly small cracks in ice accumulated at −20 °C [17]

perpendicular to the cylinder axis. Thin sections prepared from the ice accumulated at −6 °C show similar grain structure. However, in this case, the ice grows more slowly resulting in somewhat bigger columnar grains (Fig. 3b). In the thin section perpendicular to the cylinder axis for the atmospheric ice accumulated at −20 °C (Fig. 3c), the columnar structure is not nearly as apparent due to the smallness of grains and the high freezing rate.

For more information about the grain structure of these three types of atmospheric ice, see Kermani [21].

Results of cyclic load and discussion

Results of the tests in the first scenario

The individual and averaged values of bending strength of atmospheric ice accumulated at −6, −10, and −20 °C, and tested under cyclic load at various test temperatures are recorded in Table 1. The points of static loading in this table indicate the average of at least five tests at strain rate of 2×10^{-3} s^{-1}, reported in Kermani et al. [4]. According to the guidelines recommended by the IAHR working group on test methods [20], loading times to failure in the order of 1 s, yield satisfactory results in measurement of bending strength of ice under static loading. In Kermani et al. [4], this corresponds to a strain rate of 2×10^{-3} s^{-1}. Figure 4 shows the configuration of this cyclic test. Some typical stress-time and force-beam deflection graphs during the first and second scenarios, as well as static loading are shown in Figs. 5 and 6a, b, c.

Bending strength σf during cyclic loading was calculated from the beam theory using the equation:

$$\sigma f = \frac{6FL}{wh^2}$$

where F is the failure load; L is the length of the beam; w and h are width and height of the beam, respectively, measured at the failure plane.

Figure 7 shows the comparative results of bending strength of ice accumulated at −10 °C and tested at different temperatures under both the static and cyclic loads. The difference between flexural behavior of atmospheric ice under these two loading modes is distinguishable in that figure. As reported by Kermani et al. [4], the strength of atmospheric ice under static loading appears to increase with decreasing test temperature at the lower strain rates (less than 2×10^{-3} s^{-1}). This trend has also been reported by Gagnon and Gammon [9] for iceberg ice and by Gow and Ueda [8] for freshwater ice. As seen in Fig. 7, at higher strain rate, little or no temperature effect on bending strength of atmospheric ice is observed. The bending strength of ice under cyclic load, however, decreases with decreasing in test temperature. There are very few studies

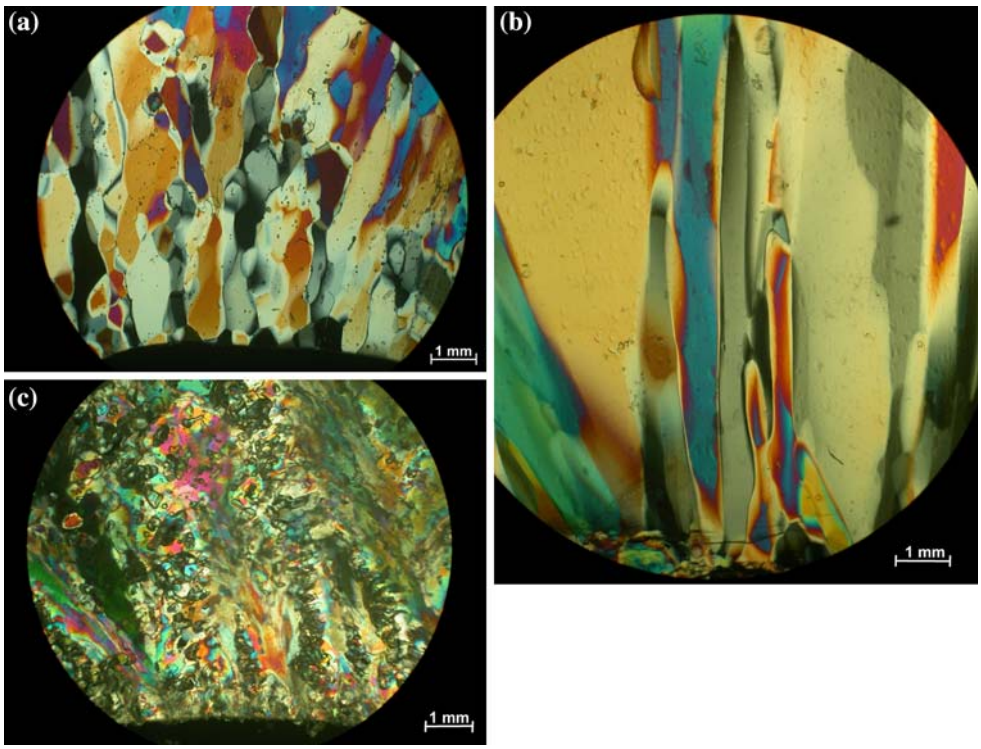

Fig. 3 Thin section (perpendicular to the cylinder axis) showing grains near the cylinder surface (bottom) in atmospheric ice accumulated at **a** −10 °C, **b** −6 °C, **c** −20 °C [21]

Table 1 Results of bending stress at failure in cyclic load (the first scenario) on ice accumulated at −6, −10, and −20 °C and tested at various temperatures

Row	Bending strength under cyclic load in the first scenario (MPa)				
	$T_a = -10$ °C $T_t = -3$ °C	$T_a = -10$ °C $T_t = -10$ °C	$T_a = -10$ °C $T_t = -20$ °C	$T_a = -6$ °C $T_t = -6$ °C	$T_a = -20$ °C $T_t = -20$ °C
1	3.26	1.75	2.81	2.95	1.94
2	2.30	2.75	2.41	2.88	1.86
3	2.77	3.21	1.98	2.96	1.46
4	2.71	2.75	2.57	3.33	1.73
5	3.23	2.11	3.46	3.53	1.93
6	2.97	2.83	2.08	2.18	1.18
7	2.62	3.50	2.42	2.72	1.70
8	2.23	2.36	2.51	3.22	1.34
9	2.51	2.95	2.47	2.87	1.24
10	2.16	3.30	1.92	1.59	1.31
11	2.49	2.70	2.21	1.63	1.67
12	2.95	2.52	2.24	2.70	1.75
13	3.55	2.07	2.28	2.45	1.21
14	2.92	2.39	2.06	2.50	–
15	–	–	2.69	–	–
16	–	–	2.63	–	–
Average	2.81	2.66	2.44	2.68	1.56
SD	0.33	0.5	0.37	0.57	0.28
Average in static loading	2.73	2.74	2.82	2.54	1.97
SD in static loading	0.31	0.59	0.46	0.35	0.43

T_a = Accumulation temperature, T_t = Test temperature

on the effect of test temperature on bending strength of ice under cyclic loads. Nixon and Smith [13] performed cyclic loading tests on freshwater ice subjected to reverse bending using a driving insert of stainless steel shaft with wooden "paddle wheels" fitted on the end of the shaft. The ice was molded on the insert and the wood, and tested at −7, −13,

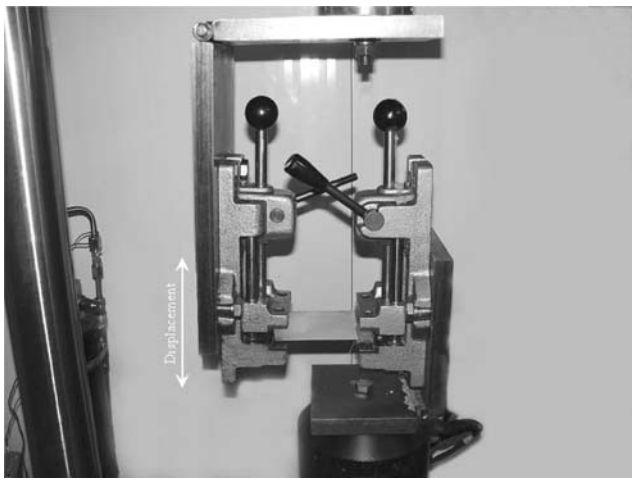

Fig. 4 Configuration of cyclic load tests

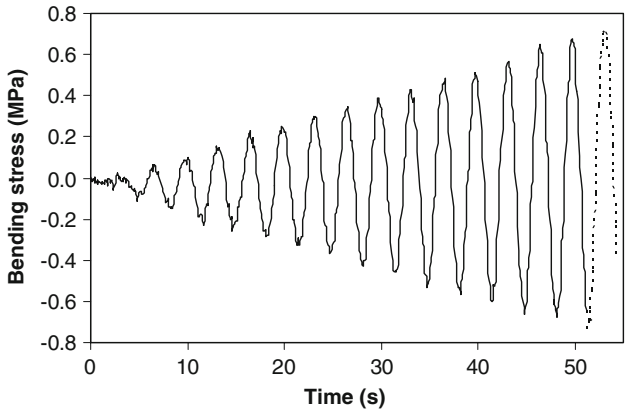

Fig. 5 A typical stress-time graph in first test scenario (Load frequency = 0.3 Hz)

−18, and −30 °C. In their tests, cyclic loads less that 40% of the monotonic failure load were applied. According to their results, fatigue life for a given load increased as temperature decreased though the difference in lifetime between tests at −7 and −13 °C was reported to be negligible for lives greater than 10^4 cycles. That behavior was attributed to the test conditions giving rise to deformation by power law creep, which does not apply to gradually increasing cyclic load as is the case in the present study. As a matter of fact, some studies showed that there are more active crack nucleation mechanisms at colder temperatures than warmer ones. Gold [24], in his investigations on columnar-grain ice stated that at very low temperatures and high strain rates, elastic anisotropy leads to stress concentrations and becomes an important mechanism for crack nucleation. The crack nucleation mechanisms, flaws, microcracks, and other defects are more effective in cyclic loads because the reversing bending stress provides identical opportunities for the cracks and cavities at both the top and bottom of the neutral axis of the ice beam to propagate and cause beam fracture. This is not the case for static loading where the cavities and cracks at the top of the beam are always under compression and in fact don't have any effect on the ice fracture.

As seen in Fig. 7, at two out of three test temperatures, the bending strength of atmospheric ice under cyclic load is less than its value under static load. This reduction has been reported by many other investigators (e.g. Haskell et al. [14], Haynes et al. [12], Kerr [25]).

The difference between the results of bending strength of ice accumulated at −10 °C and tested at −3 °C under cyclic and static load can be attributed to three possible causes: the inherent scatter in results of bending strength of ice under both cyclic and static loads; the ductility of atmospheric ice at temperatures close to melting point, causing finer and less microcracks in each loading cycle than at colder temperatures; and finally, the healing of microcracks at warmer temperatures. Gold [26, 27] has focused on the evolution of microfractures in ice and their effect on creep and fracture. When the fracture-generating stresses are removed, small fractures tend to change into spherical inclusions and lose their weakening effect. Thus, when stresses are repeatedly applied and removed, the formation of microfractures will not weaken the ice as much if the fracture can heal during the time between stress applications. While the magnitude and cycling of the applied stress depends on conditions unrelated to the ice itself, the time for healing of microfractures depends on the size of the nucleated crack, the presence or absence of air in the crack, the ice temperature, and the applied temperature gradient. Colbeck [28] described the thermodynamics of cracks in ice and developed a model supported by experimental tests to calculate the rate of crack healing in ice. He concluded that the small cracks at warmer temperatures heal more rapidly than at colder temperatures. It means that at higher temperatures, where cracks heal more easily, ice shows more resistance against failure.

Figure 8 compares the flexural strength of three types of atmospheric ice under cyclic and static loads. For static load, it is observed that the flexural strength of atmospheric ice accumulated at −20 °C and tested at the same temperature is lower than that of the two other types despite finer grain size. The reason for these differences is the presence of a significant number of cavities in the ice accumulated at −20 °C which are susceptible to stress concentration. These cavities play the same role in weakening this type of atmospheric ice under cyclic load. However, as mentioned previously, they are more effective in cyclic load because of the reversing bending stress.

The flexural strength of the ice accumulated at −10 °C under static load is higher than that of the two other ice types. The smaller grain size of this ice, as compared to that of ice accumulated at −6 °C, as well as the colder test temperature

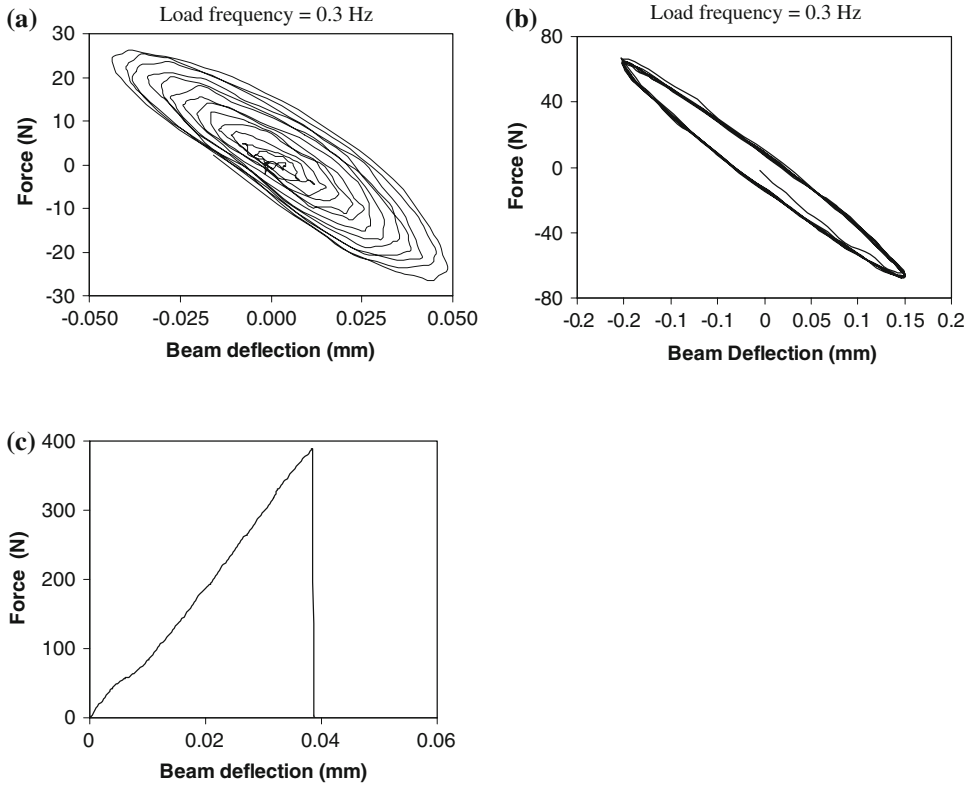

Fig. 6 Typical force-beam deflection curves with sample of atmospheric ice accumulated at −10 °C and tested at the same temperature **a** First scenario (cyclic load with increasing stress amplitude) **b** Second scenario (constant amplitude cyclic load) **c** Static load using three-point-beam test

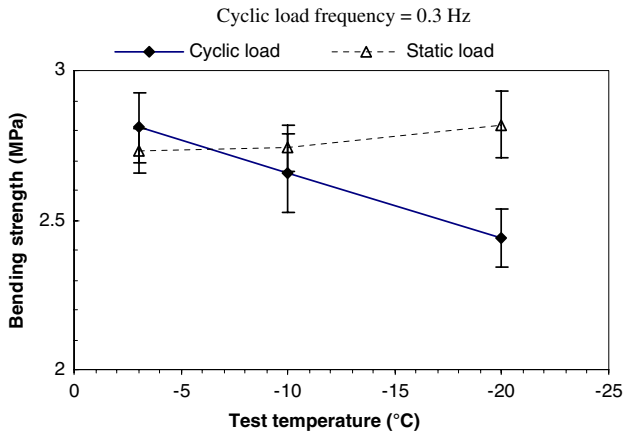

Fig. 7 Bending stress at failure for atmospheric ice accumulated at −10 °C and tested at various temperatures under cyclic and static loads in the first scenario

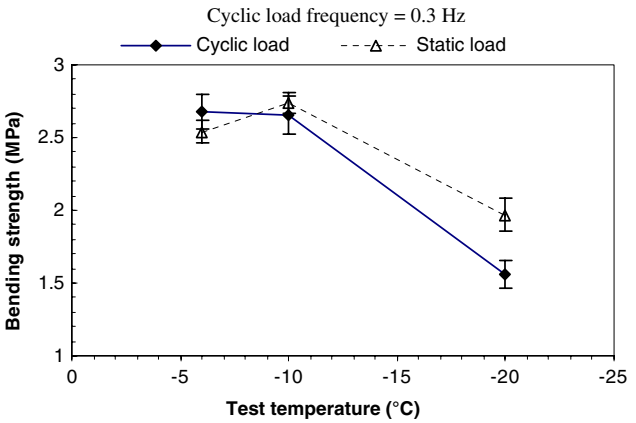

Fig. 8 Flexural strength of atmospheric ice accumulated and tested at various temperatures under cyclic and static loads in the first scenario

(−10 °C) explains its higher flexural strength. The lack of cavities in ice accumulated at −10 °C compared to the many cavities in ice accumulated at −20 °C, despite the warmer test temperature and coarser grains, results in a stronger structure and higher flexural strength for the former. As mentioned before, the bending strength of atmospheric ice accumulated at −10 °C and tested at the same temperature under cyclic load is slightly lower than that under static load due to the weakening effect of cyclic loads.

The bending strength of atmospheric ice accumulated at −6 °C and tested at the same temperature under cyclic load is slightly higher than that under static loads because of the three reasons mentioned previously for the ice accumulated at −10 °C and tested at −3 °C. It is worthwhile to note that despite the finer grains of the ice accumulated at −10 °C, the bending strength of this type of ice under cyclic load is approximately equal to the one of the ice accumulated at −6 °C.

Results of the tests in the second scenario

Results of the tests with constant amplitude cyclic load during the second scenario are given in Table 2. The

samples of atmospheric ice were subjected to a sinusoidal loading. The stress magnitude was set at four different values, and five tests were performed therein. Weber and Nixon [15] investigated the cyclic crack growth in S2 columnar freshwater ice during loading of a notched beam in four-point bending test. In their experiments, regardless of maximum stress, nearly all of the fatigue crack growth occurred during the first 1000–1500 cycles. Nixon and Smith [13], in their investigation on freshwater ice, reported a life of about 500 cycles for the cyclic loads with amplitude of 40% of the static failure load. They reported that a small reduction in load produced a significant increase in the number of cycles to failure. Since the frequency of cyclic load in the present study was very low (0.3 Hz), and since three out of four stress amplitudes in our tests were higher than 40% of static failure load, the maximum number of cycles in this study was confined to 2000. Furthermore, the main purpose of this paper is the study of ice fracture under cyclic loads during galloping, which rarely lasts more than 2000 continuous cycles.

In order to evaluate the resistance of the ice against cyclic load at a given test temperature, the tests with higher stress amplitude were performed first. At a given stress amplitude and test temperature, when no sample had failed after 2000 cycles, it was assumed that the ice does not fail at lower amplitudes. Since −10 °C is a typical wintertime temperature in Quebec, all four stress amplitudes were applied on atmospheric ice accumulated and tested at that temperature. During these tests, when the ice failed in the first or second cycle, the test result was discarded because the fracture was due to stress beyond the ice strength limit, and not as a result of low-cycle fatigue crack propagation. Owing to the inherent scatter in ice strength values, that happened several times during this investigation.

Failure usually occurred quickly and sometimes a few cycles after occurrence of the first crack. In some cases, a crack appeared at the top (or bottom) of the ice beam but did not propagate all through the specimen cross-section (Fig. 9). In these cases, the tests were continued until complete failure of the specimens.

In the Table 2, it is observed that at test temperatures of −10 °C and warmer ones (−3 and −6 °C), low amplitude loads (i.e. less than 2.5 MPa) do not cause premature ice fracture. These low amplitude stresses develop in atmospheric ice on the cables during aeolian vibration or galloping due to low-speed winds. However, the bending stress of 2.5 MPa (at test temperature of −10 and −20 °C) is very close to the bending strength of ice [4]. As a result, several failures occurred with cyclic load in the second scenario at this stress amplitude. As mentioned previously, ice shows less resistance against crack nucleation at colder temperatures (i.e. −20 °C). This can provide more opportunities for crack propagation under cyclic loads. Furthermore, the fracture toughness of atmospheric ice accumulated at −20 °C and tested at its accumulation temperature is less than the two other types [29]. That is

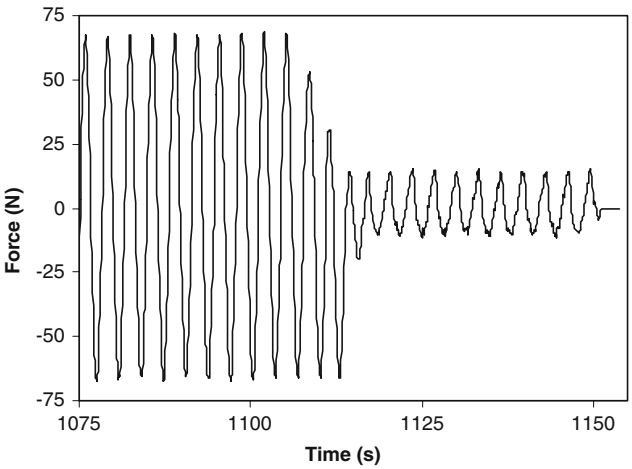

Fig. 9 Fracture of ice specimen a few cycles after occurrence of the first crack in second test scenario (Load frequency = 0.3 Hz)

Table 2 Results of low-cycle fatigue test on ice accumulated at −6, −10, and −20 °C, and tested at various temperatures in the second scenario

Accumulation and test temperature (°C)	Applied Stress (MPa)	Number of samples	Number of failed samples	Cycles to failure
$T_a = -10$	2	5	0	–
$T_t = -3$	2.5	5	2	932, 252
$T_a = -10$	1, 1.5, 2	15	0	–
$T_t = -10$	2.5	5	2	31, 6
$T_t = -20$	1	5	0	–
$T_a = -10$	1.5	5	3	1224, 331, 16
	2	5	4	360, 117, 52, 12
$T_a = -6$	2	5	0	–
$T_t = -6$	2.5	5	2	105, 405
$T_a = -20$	1	5	2	32, 12
$T_t = -20$	1.5	5	5	454, 430, 123, 58, 23

T_a = Accumulation temperature, T_t = Test temperature

why at this cold test temperature (−20 °C) both types of atmospheric ice (accumulated at −10 and −20 °C) failed after a few 100 cycles even at lower stress amplitudes. These tests showed again the vulnerability of atmospheric ice accumulated at −20 °C to cyclic loads arising from the presence of cavities and cracks in that ice. This observation is in agreement with the results of Nixon and Smith [13] on the dependency of fatigue life on defects in the ice. It is evident in Table 2 that two other types of atmospheric ice (accumulated at −6 and −10 °C) show more resistance against low-cycle fatigue crack propagation owing to fewer defects in their structure.

In order to understand the fatigue behavior of atmospheric ice under constant amplitude cyclic loads and obtain comprehensive information to establish a relationship between stress amplitude and life expectancy of an ice specimen, further investigations are required with longer test duration.

Summary and conclusions

The flexural strength of different types of atmospheric ice under cyclic load was measured using the cantilever beam approach. The ice was accumulated on a rotating cylinder in the CIGELE atmospheric icing wind tunnel at accumulation temperatures of −6, −10, and −20 °C, liquid water content of 2.5 g m^{-3} and wind speed of 10 m s^{-1}. The ice accumulated at −10 °C was tested at −3, −10, and −20 °C. The accumulated ice at −6 and −20 °C was tested at the same temperature as accumulated. More than 70 tests were carried out to measure the flexural strength of atmospheric ice under gradually increasing cyclic load and the following conclusions were obtained:

(1) The average bending strength of atmospheric ice under cyclic load for the ice accumulated at −10 °C and tested at −3, −10, and −20 °C was obtained to be 2.81, 2.66, and 2.44 MPa, respectively.
(2) This test on atmospheric ice accumulated at −6 and −20 °C and tested at the same temperature yielded the average bending strength of 2.68 and 1.56 MPa, respectively.
(3) At colder temperatures, the flexural strength of the ice under cyclic load is lower compared to that under static load.
(4) The bending strength was also found to decrease with decreasing test temperature.
(5) The flexural strength of atmospheric ice slightly increases at test temperatures close to melting point (−3 and −6 °C). This can be due to the inherent scatter in the bending test results, to the ductility of the ice at warmer temperatures, and to a possible crack healing mechanism.
(6) The flexural strength of atmospheric ice accumulated at −20 °C is less than the ice accumulated at −6 and −10 °C, owing to the presence of cracks and cavities in that ice. These cavities and cracks increase the susceptibility of that ice to prematurely fracture by providing the stress concentration necessary for that.

In order to study the effects of a constant and repetitive load on resistance of ice against crack propagation and fracture, 65 tests were conducted. The atmospheric ice accumulated at −6 and −10 °C had longer life under this constant amplitude low-cycle fatigue test. The fatigue behavior of atmospheric ice needs further investigation with longer test duration to be fully understood.

Acknowledgements This work was carried out within the framework of the NSERC/Hydro-Quebec/UQAC Industrial Chair on Atmospheric Icing of Power Network Equipment (CIGELE) and the Canada Research Chair on Engineering of Power Network Atmospheric Icing (INGIVRE) at Université du Québec à Chicoutimi. The authors would like to thank the CIGELE partners (Hydro-Québec, Hydro One, Réseau Transport d'Électricité (RTE), and Électricité de France (EDF), Alcan Cable, K-Line Insulators, Tyco Electronics, CQRDA, and FUQAC) whose financial support made this research possible.

References

1. Javan-Mashmool M, Volat C, Farzaneh M (2005) A theoretical model for measuring stress induced by a vibrating load at ice/material interface. In: Proceedings 11th international workshop on atmospheric icing of structures, Montreal, pp 141
2. Eskandarian M (2005) Ice shedding from overhead electrical lines by mechanical breaking. Ph.D. Thesis, University of Quebec at Chicoutimi
3. Jamaleddine A, McClure G, Rousslet J, Beauchemin R (1993) Computers and Structures 47(4–5):523
4. Kermani M, Farzaneh M, Gagnon RE (2008) Cold Reg Sci Technol 53(2):162
5. Timco GW, Frederking RMW (1982) Cold Reg Sci Technol 6:21
6. Frederking RMW, Svec OJ (1985) Cold Reg Sci Technol 11:247
7. Dempsey J P, Wei Y, DeFranco S, Ruben R, Frachetti R (1989) Fracture toughness of S2 columnar freshwater ice: crack length and specimen size effects—Part1. The eighth international conference on offshore mechanics and arctic engineering, pp 83
8. Gow JA, Ueda TH (1988) Cold Reg Sci Technol 16:249
9. Gagnon RE, Gammon PH (1995) J Glaciol 41(137):103
10. Kim H, Keune JN (2007) J Mater Sci 42(8):2802. doi:10.1007/s10853-006-1376-x
11. Gagnon RE (2008) High-speed imaging of mechanisms responsible for sawtooth cyclic loading during ice crushing. In: Proceedings of 19th IAHR international symposium on ice, Vancouver, British Columbia, Canada
12. Haynes FD, Kerr AD, Martinson CR (1993) Cold Reg Sci Technol 21:257
13. Nixon WA, Smith RA (1986) J Phys Coll CI 48(Suppl 3):329
14. Haskell TG, Robinson WH, Langhorne PJ (1996) Cold Reg Sci Technol 24:167
15. Weber LJ, Nixon WA (1997) Cold Reg Sci Technol 26:153
16. Nixon WA, Weber LJ (1991) Ann Glaciol 15:236

17. Kermani M, Farzaneh M, Gagnon RE (2007) Cold Reg Sci Technol 49:195
18. Kollár LE, Farzaneh M (2009) Atomization Spray 19(4):389
19. Stallabrass JR (1978) An appraisal of the single rotating cylinder method of liquid water content measurement. National Research Council of Canada, Division of Mechanical Engineering, Rep. LTR-LT-92
20. Schwarz J, Frederking R, Gavrillo V, Petrov I, Hirayama K, Mellor M, Tryde P, Vaudrey K (1981) Cold Reg Sci Technol 4:245
21. Kermani M (2007) Ice shedding from cables and conductors—a model of cracking activity of atmospheric ice in brittle regime. Ph.D. Thesis, University of Quebec at Chicoutimi
22. Bolotin VV (1999) Mechanics of fatigue. CRC Press, Washington DC
23. Laforte JL, Phan L (1983) J Climate and Appl Meteorology 22(7):1175
24. Gold LW (1972) Philos Mag A 26(2):311
25. Kerr AD (1976) J Glaciol 17(76):229
26. Gold LW (1960) Can J Phys 38:1137
27. Gold LW (1967) Time to formation of first cracks in ice, in physics of snow and ice: International conference. Sappora, Japan, vol 1, Part 1, pp 359
28. Colbeck SC (1986) Acta Metall 34(1):89
29. Kermani M, Farzaneh M. (2008) Fracture toughness of atmospheric ice. In: Proceedings of 19th IAHR International Symposium on Ice, Vancouver, British Columbia, Canada